Journal of Electroceramics 4:S1, 135–140, 1999

Electrolytic Formation and Morphology of Biomimetic Apatite Coatings

H. MONMA, O. NEMOTO, S. TAKAHASHI & H. KOBAYASHI
Faculty of Engineering, Kogakuin University, 2665 Nakano-cho, Hachioji, Tokyo, 192 Japan

Submitted November 14, 1997; Revised November 13, 1998, Accepted November 2, 1998

Abstract. Calcium-deficient apatite has been cathodically deposited on SUS stainless steel from an acidic calcium phosphate solution. The resulting apatite porous coatings were characterized morphologically, compositionally and structurally. The porous coatings were modified into dense coatings by immersion in an aqueous supersaturated calcium phosphate solution.

Keywords: apatite, electrodeposition, calcium phosphates

1. Introduction

Hydroxyapatite (HAp) is a compound with acomposition of stoichiometric $Ca_{10}(PO_4)_5(OH)_2$ and calcium-deficient $Ca_{10-x}(HPO_4)_x(PO_4)_{6-x}(OH)_{2-x} \cdot nH_2O$; $0 < x \leq 1$. Calcium-deficient HAp resembles biological HAp and has become of interest as well as the conventional stoichiometric HAp bioceramics. HAp coatings have been extensively studied for the bioactive surface treatment of bioinert metals and ceramics, because of the attractive biocompatibility of HAp with living tissues [1, 2]. Many HAp coating methods have been developed, e.g., plasma-spraying, sputtering, spark discharge in an electrolyte, spontaneous deposition from a calcium phosphate solution, electrophoresis, electrodeposition, dipping-pyrolysis, spray-pyrolysis and so forth. The authors noted simplified processing associated with the cathodic electrodeposition method [3–6], and have characterized the electrodeposits [7–11]. Cathodic deposition occurs in acidic calcium phosphate solutions through the following reactions on and near the cathode.

$$H_2O + e^- \rightarrow OH^- + 1/2H_2\uparrow \quad (1)$$

$$H_2PO_4^- + OH^- \rightarrow HPO_4^{2-} + H_2O \quad (2)$$

$$10\,Ca^{2+} + 6\,HPO_4^{2-} + 2\,OH^- \rightarrow HAp\downarrow + 6\,H^+ \quad (3)$$

$$H^+ + e^- \rightarrow 1/2H_2\uparrow \quad (4)$$

In the present study, electrodeposited HAp coatings with porous micro-structures were characterized, and modified into dense structures by immersion in an aqueous supersaturated calcium phosphate solution.

2. Experimental

HAp electrodeposition runs were carried out by electrolyzing 0.2 mol/dm^3 $Ca(H_2PO_4)_2 \cdot H_2O$ (monocalcium phosphate monohydrate, referred to as MCP) solutions (50 ml) with $NaNO_3$ (7.0 g) and NaF(0.05 g) added at constant cathode currents *(Dc)*, temperatures and electrolysis times. The former additive is used for increasing the electrolyte conductivity and the latter for assisting the HAp formation, respectively. Figure 1 shows the electrolysis assembly. The resulting deposits on the cathode were washed with distilled water, dried in air, and examined by *X*-ray diffractometry (XRD), Fourier transform infrared spectroscopy (FTIR), scanning electron microscopy (SEM) equipped with an energy

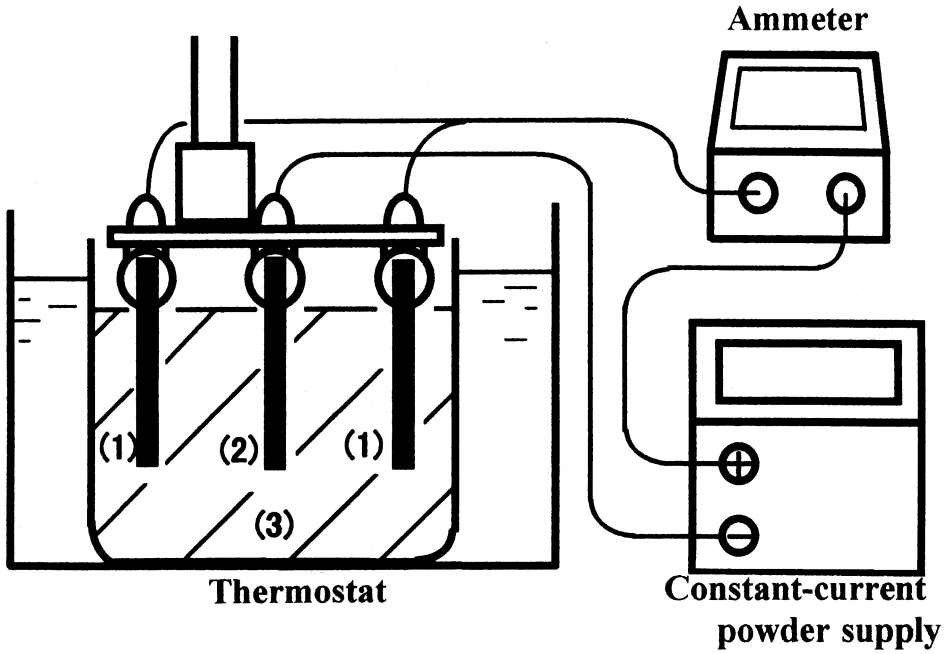

Fig. 1. Galvanostatic electrolysis cell for cathodic HA_p deposition. (1): Pt anode (2): SUS stainless steel cathode (3): MCP solution with $NaNO_3$ and trace NaF

dispersive spectrometer (EDX), and in part by transmission electron microscopy (TEM). The microstructural modification of as-deposited HAp porous coatings was conducted by immersion at 37°C in a simulated body fluid [12] which is a saturated calcium phosphate solution with respect to HAp (SBF-treatment).

3. Results and Discussion

3.1. Morphology and Structure

Figure 2 shows morphological changes of HAp deposits with electrolysis time (A-C) and a TEM image of an HAp grain and its electron diffraction image (*D*). The formation of such unique rounded grains might be related to the nucleation and growth of HAp in a restricted zone near and parallel to the cathode, i.e., in a narrow zone with steep gradients of pH and ion concentrations induced by the above mentioned cathodic reactions. The shapes of HAp grains varied with increasing electrolysis time, i.e., ellipsoidal rod with conical heads → hexagonal pyramidal rod with point heads → hexagonal pyramidal rod with flat ends. Finally, it must grow to the hexagonal prismatic rod form usually observed for apatite single crystals. The TEM pattern showed that the grain is an apatite single crystal elongated in the [001] direction and surrounded with the (100) planes of the apatite structure.

3.2. Composition and Calcium-deficiency

Figures 3 and 4 show XRD patterns and FTIR spectra of HAp layers before and after heating, respectively. The formation of a mixture of apatite and β-$Ca_2P_2O_7$ at 800°C indicated that the as-prepared HAp had a calcium-deficiency with a Ca/P molar ratio less than the stoichiometric ratio 1.67. The bands between 1100 and 1000 (ν_3), 960 (ν_1), 600 (ν_4), 570 (ν_4) and 470 cm^{-1} (ν_2) are assigned to the vibrations of apatitic PO_4^{3-}, and at 860 cm^{-1} to P-OH of HPO_4^{2-} partially substituting PO_4^{3-} in apatite. Although CO_3 in apatite has a band near 860 cm^{-1}, the absence of a band at 1550–1400 cm^{-1} suggests that CO_3 is absent. No bands due to O-H in HAp (stretch: 3570 cm^{-1}, libration: 630 cm^{-1}) suggested that the OH sites were

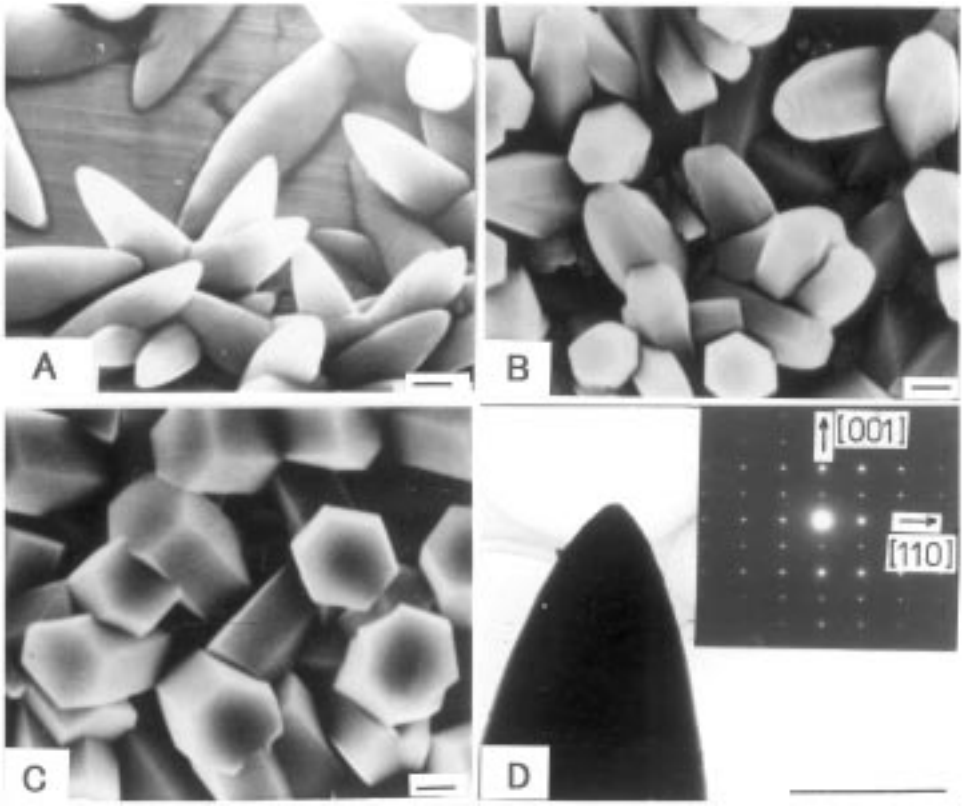

Fig. 2. Morphological changes of HAp crystals with electrolysis time (A-C), TEM image and electron diffraction (D). – : 2 μ m
A : Dc = 6mA/cm$_2$, 80°C, 2 min B : Dc = 6mA/cm$_2$, 80°C, 15 min, C : Dc = 2mA/cm$_2$, 80°C, 60 min, D : Dc = 6mA/cm$_2$, 90°C, 5 min.

appreciably occupied by F ions and/or H_2O molecules. The substitution by F ions was confirmed by the appearance of a band at 3540 cm^{-1} at 800°C, which is characteristic of OH in partially fluoridated HAp [13]. The band at 723 cm^{-1} and many bands around 1210–1160 cm^{-1}, which appeared at 800°C, are assigned to P_2O_7. The appearance of OH by heating suggested thermal reactions in the solid, such as $PO_4 + (F, H_2O) \rightarrow HPO_4 + (F, OH) \rightarrow 1/2P_2O_7 + (F, OH) + 1/2H_2O\uparrow$ [14]. Figure 5 shows EDX spectra for a HAp single crystaland a synthetic standard. Elements Ca, P and a trace of Na were detected. The Ca/P ratio of the crystal was estimated to be ca. 1.4 which was a little less than 1.50 corresponding to $x = 1$ of the calcium-deficient formulae. This means that Na^+ substitutes in low levels for Ca^{2+}. Consequently, the composition of electrodeposited HAp is expressed as $(Ca, Na)_{10-x}(HPO_4)_x(PO_4)_{6-x}(OF, OH, H_2O)_2$.

3.3. Modification of HAp Porous Coatings

The microstructure of the as-deposited HAp coatings was porous due to the reduction of H_2O accompanying the generation of H_2 gas. We tried to convert the porous into dense coatings by immersion in the SBF. Figure 6 shows the weight changes of the as-deposited HAp coatings after immersion. The phase of the coatings after the immersion was confirmed to be only apatite by XRD. The observed weight increases thus represent additional deposition of apatite from the SBF. The larger the as-deposited amount, the more easily additional precipitation of HAp occurred. Figure 7 shows the microstructural comparison between as-deposited and SBF-treated HAp coatings. The morphologies of the modified dense structures were very similar to those formed spontaneously on substrates with silanol groups from SBF [15]. The silanol groups are bound to the

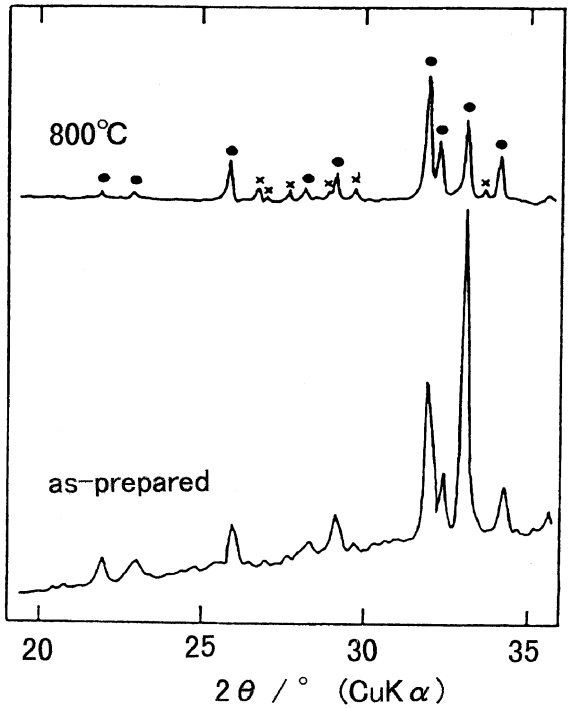

Fig. 3. XRD patterns for deposit B (ref. Fig. 2) and the heated product. ● : apatite, ×: $\beta - Ca_2 P_2 O_7$

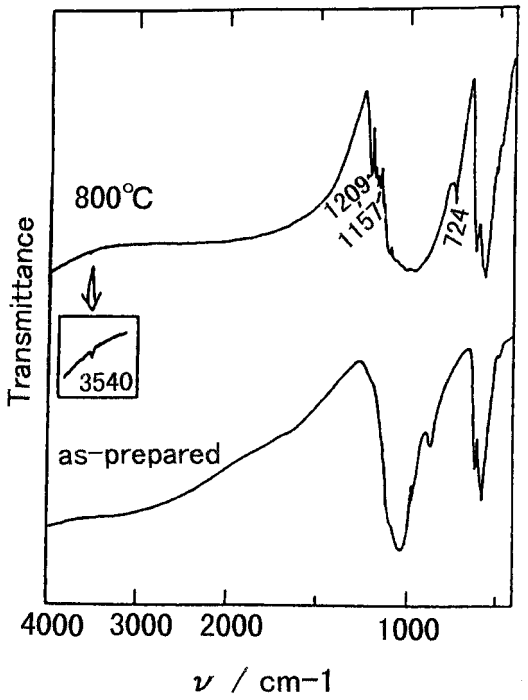

Fig. 4. FTIR spectra for deposit B (ref. Fig. 2.) and its heated product.

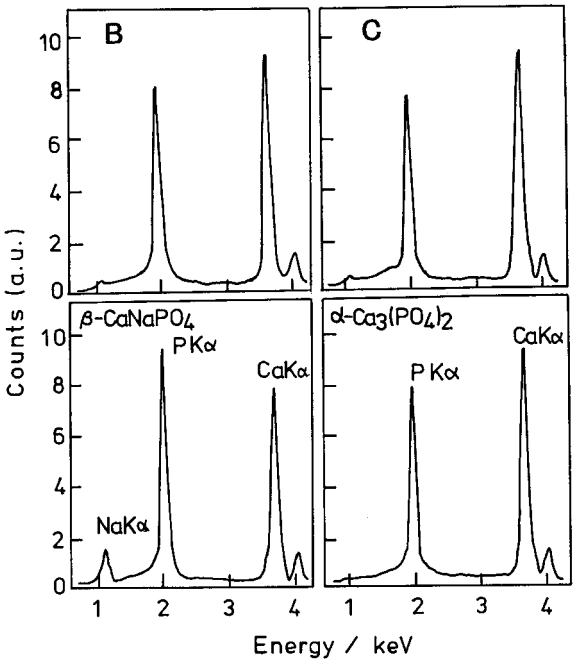

Fig. 5. EDX spectra for an HAp grain of each of deposits B and C (ref. Fig. 2) and synthetic standards.

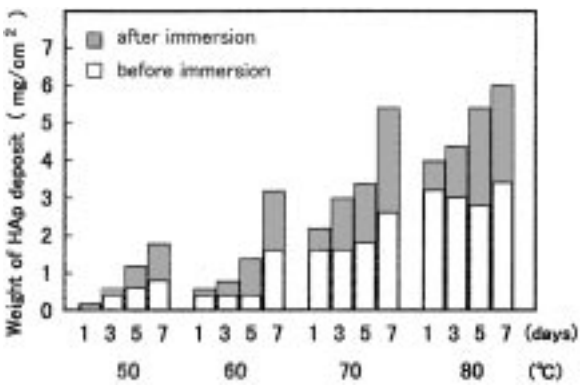

Fig. 6. Weight increases of HAp coatings after immersion in SBF at 37°C, where HAp coatings with different amounts were electrodeposited at 50 to 80°C.

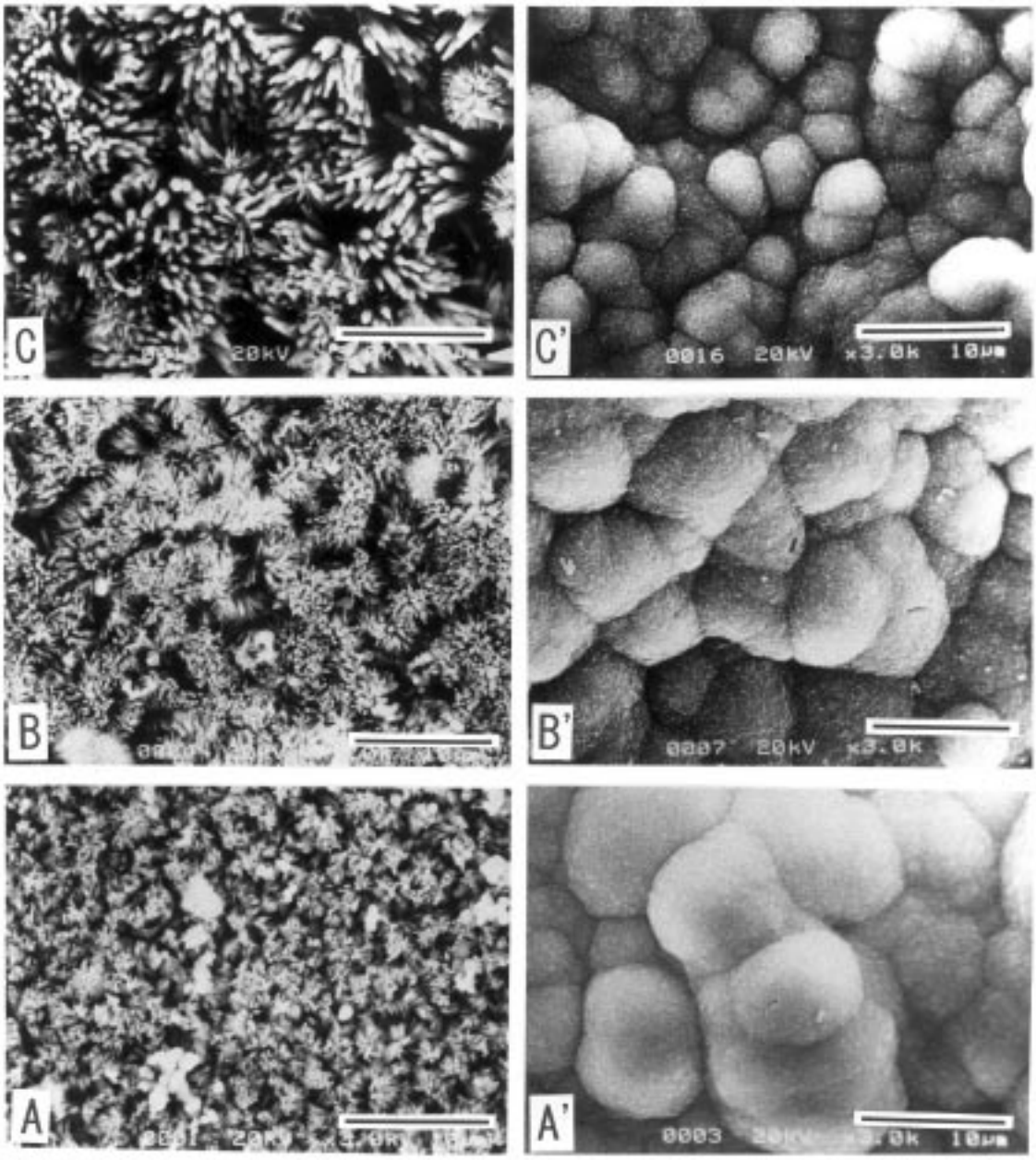

Fig. 7. Microstructures of as-deposited HAp coatings (left side) and SBF-treated HAp coatings (right side). – : 10 μm
SBF-treatment : 7 days at 37°C
A and A': deposit at 50°C and SBF-treated one
B and B': deposit at 60°C and SBF-treated one
C and C': deposit at 80°C and SBF-treated one

substrates to induce apatite nucleation. Similarly, the porous electrodeposited HAp crystals are believed to act as nuclei for the next HAp precipitation from the SBF.

4. Conclusions

1. HAp crystals with a calcium deficiency near 1.5 in Ca/P mole ratio and comparatively clear morphologies were electrolytically prepared.
2. Morphological changes with the growth were as follows: ellipsoidal rod with conical head → hexagonal pyramidal rod with pointed heads → hexagonal pyramidal rod with flat ends, and finally to hexagonal prismatic rod. Each crystal was elongated in the [001] direction and surrounded by the (100) plane of the apatite structure.
3. The porous structures of the HAp coatings were modified into dense structures by immersion in an aqueous supersaturated calcium phosphate solution due to additional HAp precipitation.

References

1. K. de Groot, *Bioceramics of Calcium Phosphate*, edited by K. de Groot (CRC press, Inc., Florida, (1983), p. 99; L. Feenstra and K. de Groot, *ibid.*, p. 115.
2. H. Aoki et al., *Bioceramics-Development and Clinical Applications*, edited by H. Aoki and J. Niwa (Quintessence, Tokyo, 1987), p. 138.
3. J. Redepenning and J. P. McIsaac, *Chem. Mater.*, **2**, 625 (1990).
4. M. Shirkhanzadeh, *J. Mater. Sci. Lett.*, **10**, 1415 (1991).
5. P. Royer and C. Rey, *Surf. Coat. Technol.*, **45**, 171 (1991).
6. S. Ban and S. Maruno, *Bioceram.*, **5**, 49 (1992).
7. H. Monma, *Phos. Res. Bull.*, **2**, 21 (1992).
8. H. Monma, *J. Ceram. Soc. Jpn.*, **101**, 737 (1993).
9. H. Monma, *J. Mater. Sci.*, **29**, 949 (1994).
10. H. Monma, S. Takahashi, and H. Kobayashi, *Key Eng. Mater.*, **111–112**, 291 (1995).
11. H. Monma, T. Kitami, and M. Tsutsumi, in *Advanced Materials '93*, edited by S. Somiya, M. Doyama, M. Hasegawa and S. Yamada (Elsevier Science B.V., Amsterdam, 1994), p. 781.
12. H.-M. Kim, F. Miyaji, T. Kokubo, and T. Nakamura, *J. Ceram. Soc. Jpn.*, **105**, 111 (1997).
13. B. Menzel and C. H. Amberg, *J. Colloid Interface Sci.*, **38**, 256 (1972).
14. H. Monma, J. Tanaka, and S. Ueno, *Gypsum & Lime*, **165**, 16 (1980).
15. S.-B. Cho, F. Miyaji, T. Kokubo, K. Nakanishi, N. Soga, and T. Nakamura, *J. Ceram. Soc. Jpn.*, **104**, 399 (1996).